26th INTERNATIONAL CONGRESS ON SOUND AND VIBRATION
7-11 July 2019, Montreal

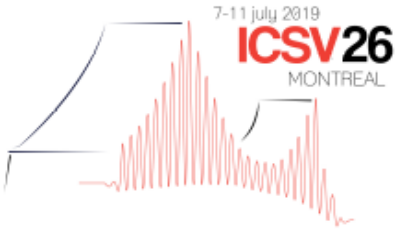

APPLICATION OF 1-NORM REGULARISATION TECHNIQUES IN ESTIMATING THE INDOOR TYRE PASS-BY NOISE CONTRIBUTION WITH THE INVERSE METHOD

Athanasios Papaioannou, Stephen Elliott, Jordan Cheer
University of Southampton, Southampton, UK
email: ap3m17@soton.ac.uk

The indoor pass-by noise measurement can nowadays be realised in a laboratory environment with a microphone array and a stationary vehicle on a rolling road, according to ISO – 362-1:2016. Within this indoor testing procedure, the different contributions from the various noise sources on a car can be estimated using an inverse method with a set of microphones close to the various sources. This work assumes a 2D-tyre model to approximate the behaviour of a real car tyre at low frequencies. The inverse method is then adopted using this model for the tyre noise contribution synthesis and corresponding source strength and synthesised pressure estimates are calculated. A novel regularisation method is finally investigated to further optimise the far field pass-by noise pressure estimates through the frequency range of interest.
Keywords: tyre noise, inverse method, l_1 regularisation

1. Introduction

The exterior sound emission of a vehicle is an increasingly important criterion for the homologation of road vehicles. Until recently, pass-by noise has been measured outdoors, but can now be measured in an indoor environment with a microphone array and a stationary vehicle on a rolling road, according to ISO-362-1:2016 [1]. In-room pass-by noise testing systems using a roller bench in a semi-anechoic room increase the total robustness and repeatability of the measurements, while there exists the ability to quantify the various car noise source contributions, which is described as the pass-by noise contribution analysis, and gives further insight into the total noise disturbance.

Pass-by noise contribution analysis is typically realised by using a set of additional microphones close to the real car sources. Each source is approximated by a set of uncorrelated point sources and an inverse method is then implemented in order to quantify the various noise source distributions [2-6]. To accomplish this inverse identification procedure, acoustic transfer responses are measured between all point sources and all microphone positions to allow full matrix coupling between all sources and indicators, while the synthesis of the acoustic pressure or power in the far field is realised by using a linear sensor array at 7.5 m away from the car. Within the work described above, the equivalent point source positions have been predefined based on the physical insight of the car source noise generating mechanisms. With the aim of overcoming this limitation, the work presented herein utilises corresponding regularisation methods that can effectively optimise the positions of the chosen equivalent point sources for the tyre pass-by noise contribution synthesis.

2. The tyre model

The tyre noise contribution is approximated herein by using a 2D linear tyre model, following the work done by Rustighi and Elliott in [7] and is presented in detail in [8]. The tyre model used is the stationary ring model, as originally proposed by Huang and Soedel [9]. In this model, the stiffness of the sidewalls, the inflation pressure and the loss factors of sidewalls, tread and internal pressure have been taken into account. However, the model only includes the vibration of the belt and it does not take into account the effects due to the rotation and the anti-symmetric rigid belt modes. The two-dimensional ring can provide a good approximation to the behaviour of a real car tyre in the low-frequency range (below about 400 Hz) given that the parameters of the model are properly tuned to the tyre characteristics.

A very simplified contact model is used which assumes that all of the contact patch is in contact with the road at all times and that only a set of isolated, locally acting springs generate the contact stiffness, which is called a Winkler bedding. In this case, the spectral density matrix for the contact forces can be calculated from a statistical model of the road roughness using a linear analysis.

The excitation of the tyre running over a rigid road profile is modelled as a random displacement distribution with a specified spatial correlation. For a vehicle travelling at a constant velocity, the displacement can be considered as a realisation of a multi-variate stationary random process and so can be described by a spectral density matrix. Each contact point travels over the same profile as that of the forward contact points, so that each point experiences, after a speed-dependent delay, the same imposed displacement.

With this model, it is possible to linearly express the relationship between road profile and tyre vibration. The spectral density matrix of the tyre's radial velocities, $\boldsymbol{S_{vv}}$, due to the road excitation can be expressed in terms of the road displacement spectral density matrix, $\boldsymbol{S_{dd}}$, as

$$\mathbf{S_{vv}} = \mathbf{T}\mathbf{S_{dd}}\mathbf{T^H} \tag{1}$$

where $\boldsymbol{T}$ is the overall transfer matrix and equal to $\boldsymbol{Y_F[I + K_{TC}C_{CT}]^{-1}K_{TC}}$, $\boldsymbol{Y_F}$ is the mobility matrix, $\boldsymbol{K_{TC}}$ a matrix describing the linear contact stiffness and $\boldsymbol{C_{CT}}$ a matrix of tyre compliances at the points in the contact patch. The radial velocity distribution around the tyre can then be calculated from the diagonal elements of $\boldsymbol{S_{vv}}$.

3. Application of inverse method to tyre pass-by noise synthesis

In this section, the formulation of the inverse method for the tyre pass-by noise contribution synthesis is given, as described in [10] for a line source.

3.1 Use of near field source estimates for far field pressure reconstruction

The model considers the tyre as a circular source of length L = 0.56 m equal to its diameter. A polar microphone array, consisting of 32 sensors, is used covering 300^0 along an arc of radius 0.65L, excluding a region of 60^0 close to the contact patch, as shown in Figure 1(a). A linear microphone array at 7.5 m away from the tyre is also used, as shown in Figure 1(b).

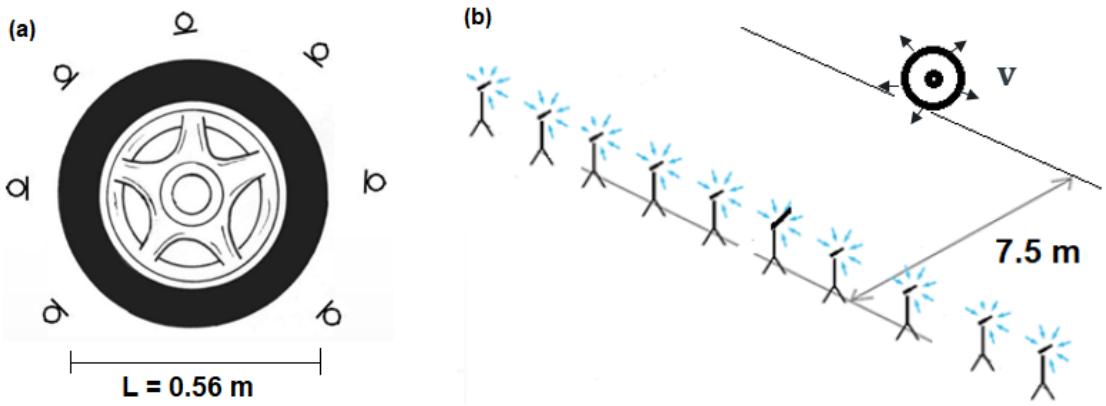

Figure 1(a): Schematic of the tyre and the polar microphone array in the near field, 2(b): Schematic of the tyre and the linear microphone array in the far field

The radiation from the tyre is approximated by using the spectral density matrix of the radial tyre velocities for a vehicle speed of 100 km/h. The matrix of pressure cross spectra at the microphones is then given by [10]

$$\mathbf{S_{pp,near}} = \mathbf{G S_{vv} G^H} \tag{2}$$

where $\boldsymbol{S_{vv}}$ is the radial tyre velocity spectral density matrix and $\boldsymbol{G}$ is the matrix of (3D free-space) Green functions, linking each radial source velocity to each pressure such that

$$\boldsymbol{G_{m,n}} = \frac{j\rho_o \omega e^{-j\omega r_{m,n}/c_0}}{4\pi r_{m,n}} \tag{3}$$

where $r_{m,n}$ is the distance from tyre element n to microphone m and c_0 is the speed of sound. To this end, the tyre source is divided into a small number of equivalent sources and the inverse method is applied to the pressure cross spectra defined in Equation 2 using the inverse (or, more generally, the pseudo-inverse $\boldsymbol{G^+}$) of the matrix of Green functions $\boldsymbol{G}$. This yields an estimate of a simplified source cross-spectral matrix, such that [10]

$$\mathbf{\hat{S}_{vv}} = \mathbf{G^+ S_{pp} G^{+H}}. \tag{4}$$

This estimate is then used to calculate the far field power spectra for a linear microphone array at 7.5 m away from the tyre, as shown in Figure 2(b). An estimate of the pressures at the sensors using the simplified source distribution is then given by

$$\mathbf{\hat{S}_{pp,far}} = \mathbf{G \hat{S}_{vv} G^H} \tag{5}$$

which can be compared to the exact directly radiated field $\boldsymbol{S_{pp,far}}$ to give a root mean square error in dB between the exact and reconstructed pressure fields averaged over all M microphones, as given by

$$\mathbf{E} = \frac{1}{\mathbf{M}} \sum_{\mathbf{m=1}}^{\mathbf{M}} \left| \mathbf{10 log_{10}} \left\{ \left| \frac{\hat{\mathbf{p}}_{\mathbf{m,m}}}{\mathbf{P_{m,m}}} \right| \right\} \right|. \tag{6}$$

where $p_{m,m}$ is the mth diagonal component of S_{pp} etc., and M is the number of microphones.

3.2 Use of L_1 – norm regularisation

In general, the conditioning of the Green function matrices and thus the accuracy of the matrix inversion in Eq. (4) is strongly dependent on the geometry of the problem. This means that it can be controlled, to a large extent, by either reducing the possible degrees of freedom in the problem [11] or by carefully choosing the optimum number and spacing of source elements as a function of frequency. In Section 3.1, the simplified equivalent source positions are predefined for a given number of elements. Therefore, this

means that the accuracy of the synthesis process can be improved by optimising the equivalent source geometry.

In this section, the optimisation of the source number and position is realised by using the sparsity – promoting properties of the l1-norm regularisation technique, widely known as the Lasso method. Within the method, the power spectral matrix of the pressure distribution $\boldsymbol{S_{pp,near}}$ is analysed with an eigenvalue factorisation [12]

$$\mathbf{S_{pp,near}} = \mathbf{VSV^H} \tag{7}$$

where $\mathbf{V}$ is a unitary matrix with the columns containing the eigenvectors $\mathbf{v}_\mu$, $\mu = 1, 2, ..., M$ and $\mathbf{S}$ is a diagonal matrix with the real non-negative eigenvalues on the diagonal. Each eigenvector represents a coherent signal across the microphones under the constraint of orthogonality. Based on the factorisation in Equation (7), the Principal Components of the pressure $\mathbf{p}_\mu$ can be calculated as

$$\mathbf{p}_\mu = \mathbf{V^H p} \tag{8}$$

These principal components represent the eigenmodes of the sound field, that is the eigenvector including its magnitude. The selection method is applied independently to each one of them and, subsequently, the output is added on a power basis since they represent incoherent parts of the sound field. In this paper, the selection method is used by only taking into account the first eigenmode for the frequency range of interest since this is found to give accurate results. The problem can therefore be described in linear matrix – vector notation as

$$\mathbf{p_1} = \mathbf{Gv_1} \tag{9}$$

where $\boldsymbol{G}$ is the Green function matrix, $\mathbf{p_1}$ is the principal component derived by the first eigenmode and $\mathbf{v_1}$ is the corresponding radial velocity component. The configuration used in this problem is more flexible, meaning that the circumference of the tyre is filled with 40 equally spaced virtual point sources. The minimised cost function is then given by

$$\mathbf{min}\|\mathbf{p_1} - \mathbf{Gv_1}\|_2^2 \ \mathbf{subject\ to}\|\mathbf{v_1}\|_1^1 \leq \boldsymbol{\delta}\,. \tag{10}$$

This convex optimisation problem is solved by using the SPGL1 toolbox [13]. The computational demand for the problem is high because no analytic solution exists. However, the utilisation of this Lasso technique gives the opportunity to choose the number of sources with which the source reconstruction is realised from a number of candidate sources. The l1 norm of the source velocity distribution promotes sparsity which is adjusted by tuning the regularisation parameter δ. The smaller the regularisation parameter δ is chosen, the more it is going to enforce sparsity in the solution and thus a smaller number of non-zero equivalent sources, but that will happen at the cost of a loss of reconstruction accuracy. The level of the regularisation parameter δ essentially provides a trade off between accuracy and the number of equivalent sources involved in the inversion.

However, the use of the l_1 regularisation at each single frequency implies the use of different equivalent source positions at different frequencies which is impractical in a real measurement campaign. Therefore, the method can be modified to choose the optimum equivalent source distribution over the frequency range of 10 to 1000 Hz. Within this procedure, the frequency range of interest is divided into $N = 200$ frequency intervals and the l_1 regularisation is performed iteratively by taking into account the l_1-norm of the radial velocity distribution associated with each distinct frequency. The minimised cost function is then given by

$$\mathbf{min}\sum_{\mathbf{i=1}}^{\mathbf{N}}\left\|\mathbf{p_{i,1}} - \mathbf{G_i v_{i,1}}\right\|_2^2 \ \mathbf{subject\ to}\ \sum_{\mathbf{i=1}}^{\mathbf{N}}\left\|\mathbf{v_{i,1}}\right\|_1^2 \leq \boldsymbol{\delta} \tag{11}$$

where the subscript i corresponds to the discrete frequencies. The final chosen equivalent source distribution is the one that delivers the minimum summed least squares error over the given frequency range.

In Section 3.3, corresponding source strength and far field pressure directivity results are presented by using the inverse method for the predefined equivalent source positions, as formulated in Section 3.1, and the l_1 regularised ones, as in Section 3.2.

3.3 Results

For values of kL = 2.57, 6.7, 10.2 (f = 200 Hz, 650 Hz and 1 kHz respectively), the near field reconstructed 4 - element source distributions and the corresponding magnitude of their reconstructed pressure directivities in the far field are given in Figure 2. In the first case (orange dots), the equivalent sources are uniformly positioned covering the whole tyre circumference, when 4, 8 or 16 equivalent sources are assumed, while for 2 sources, they are placed very close to the tread pattern. In the second case (green dots), the equivalent source positions are determined by adjusting the regularisation parameter δ until there are only 4 dominant equivalent sources at each frequency. In the third case (purple dots), the source positions are determined by performing the l_1 regularisation over the frequency range of 10 to 1000 Hz.

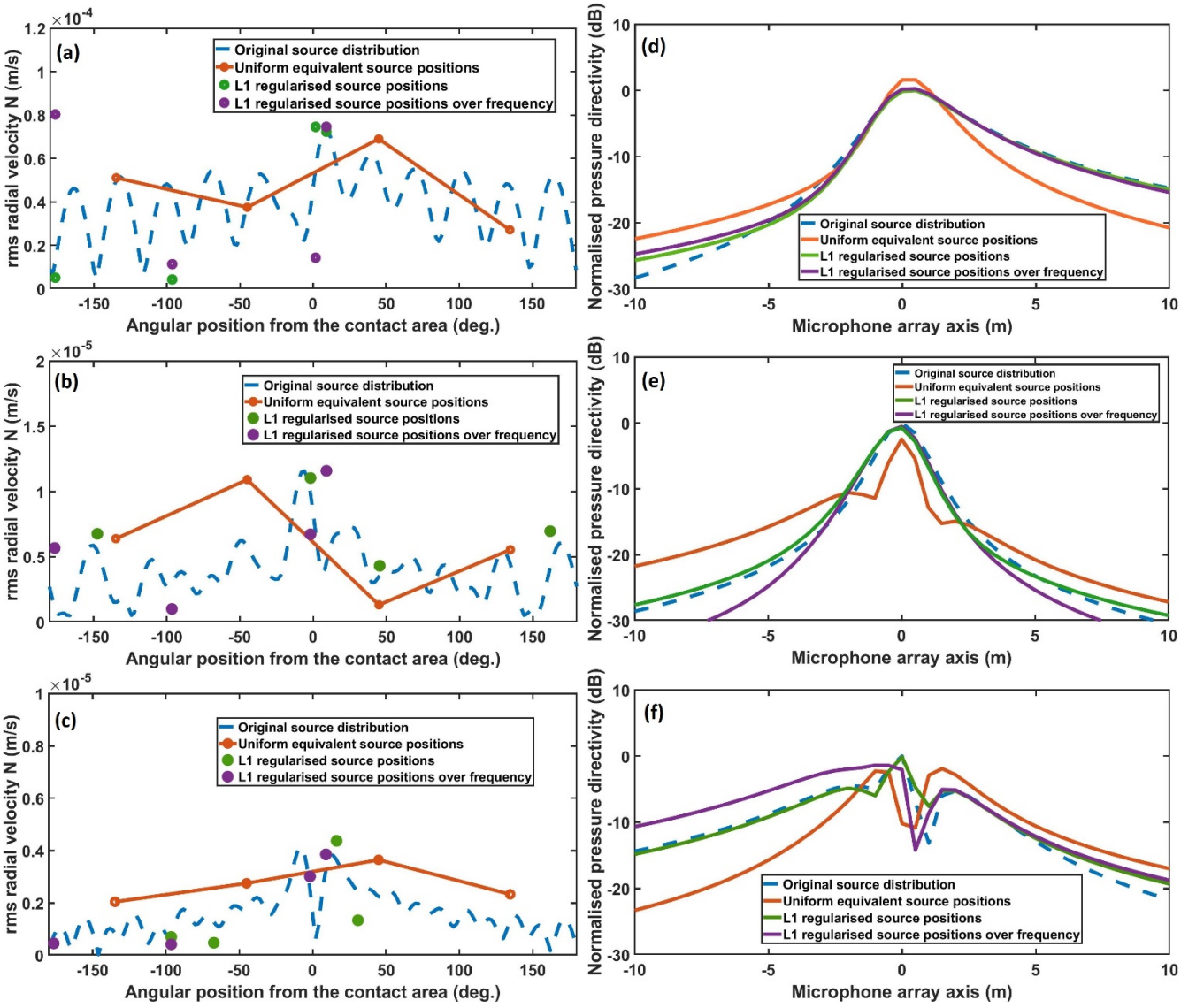

Figure 2(a), (b), (c): Comparison between original and near field reconstructed source distribution: 4 equivalent sources either chosen to give uniform spacings(orange) as in Section 3.1, chosen to give the best least squares solution (green) as in Section 3.2 or regularised over frequency (purple), 2(d), (e), (f): Comparison between direct and synthesized far field pressure directivities, kL = 2.57, 6.7 and 10.2

In Figures 2(a), (b) and (c), the original source distribution is compared with the uniformly spaced equivalent one and the l_1 regularised ones. The inverse method does not reproduce the short wavelength components of the radial velocity, but focuses on the long wavelength components. The l1-norm minimization at each single frequency chooses a different equivalent source distribution of four elements with irregular spacing compared to the uniform one. It is shown that, for the l_1 regularised source, at 200 Hz the point sources tend to group together in larger size sources as the pressure directivity results are similar if δ is adjusted to give only 3 equivalent sources. In the 650 Hz and 1 kHz cases, the point sources tend to spread out a bit more across the tyre circumference, forming smaller size sources. This phenomenon is better illustrated if the sparsity criterion is relaxed and the number of point sources is increased. At lower frequencies, a small number of block sources is then created, while at higher frequencies a larger distribution of small sources is formed, which is in accordance with the anti-aliasing spatial sampling criterion. The l1-norm minimisation over frequency gives, as projected, the same equivalent source positions for the three frequencies examined. At 200 Hz, the regularised positions over frequency are very close to the ones acquired by regularising in the single frequency, whereas, at 650 and 1000 Hz, there is a significant deviation between the equivalent source positions.

In Figures 2(d), (e) and (f), it is also shown that despite the errors in the reconstructed source distribution, the synthesised far field directivity is a good representation of the direct field because the short-wavelength components in the reconstructed source distributions, which are not reproduced with only a few equivalent sources, do not radiate efficiently into the far field. However, as frequency increases, errors in the radiated pressure far field become more apparent. The use of the l_1 regularisation at each single frequency results in an improved far field pressure directivity at the three frequencies examined here, as shown in Figure 2(d), (e) and (f), compared to the ones acquired using the uniform equivalent source distribution. The l_1-regularisation over frequency still gives an improved far field directivity compared to the uniform source one, but is, as expected, a worse representation than the one acquired at each single frequency. It is also interesting to note that, at 200 Hz, where the l_1 regularised source positions are very similar, the corresponding far field directivities are also very much alike, while, at 650 and 1000 Hz, there is a significant deviation between the curves.

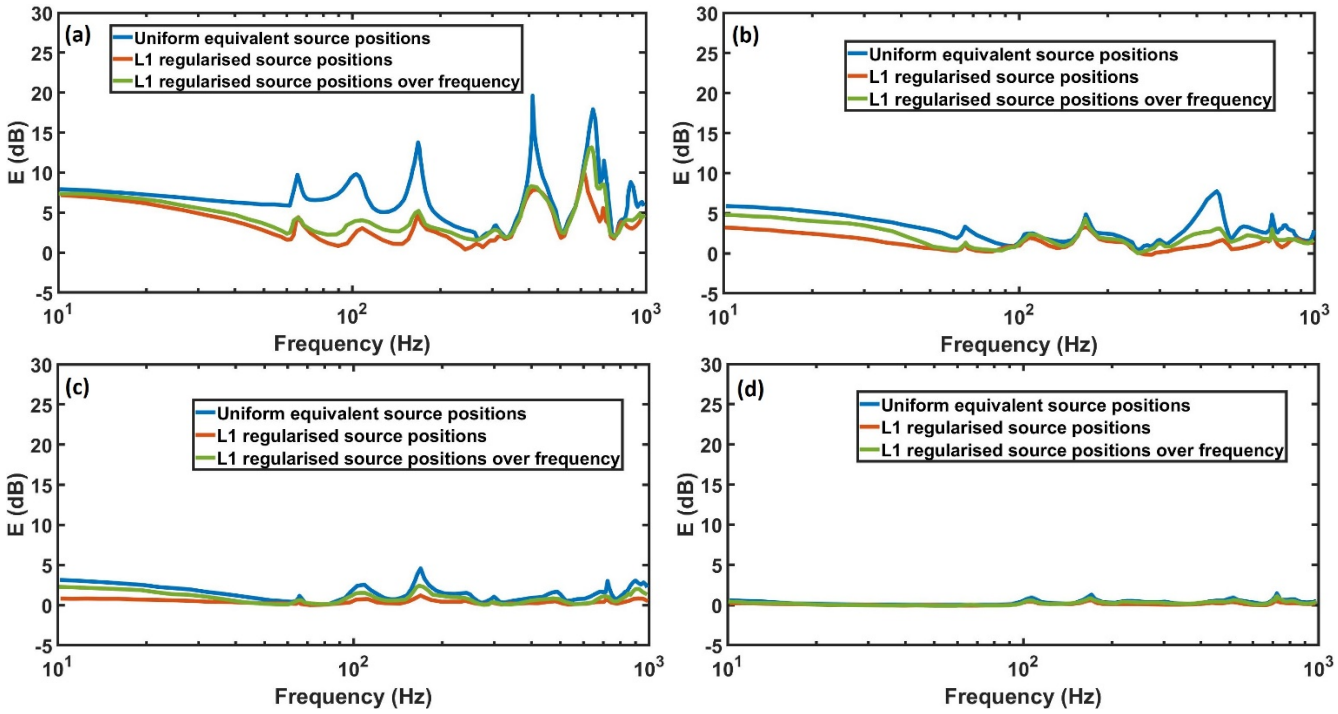

Figure 3: dB error in reconstructed far field pressures for various number of source elements: (a) 2 elements, (b) 4 elements, (c) 8 elements and (d) 16 elements chosen with the methods described in Sections 3.1 and 3.2

Figure 3(a)-(d) shows the error E in the reconstructed pressure far field as a function of frequency using a simplified source distribution of 2, 4, 8 and 16 elements respectively. As noted above, for the uniform equivalent source, in the 2-element case the source positions have been chosen to be very close to the tread pattern, while for a larger number of elements (4 and above) the source positions have been chosen uniformly spaced across the circumference of the tyre. For the l_1 regularised source, the source positions have been chosen by adjusting the regularisation parameter δ at each frequency, while, for the one regularised over frequency, the source positions are the ones that minimise the summed least squares error between 10 and 1000 Hz. It is shown that as the number of equivalent source elements increases, the error decreases correspondingly towards 0 dB which would indicate no error. The high error levels are due to the use of the ill-conditioned inverse method, associated with the conditioning of the Green function matrices. At lower frequencies, the condition number rises rapidly when the number of equivalent sources is too small and the accuracy of the inversion is subsequently limited. At higher frequencies, the conditioning of the transfer matrices improves and the errors are mostly associated with the number of equivalent sources per wavelength required for the spatial sampling criterion to be satisfied. The comparison between the errors associated with the use of the uniform and l_1 regularised source distribution shows that optimising the positions of the equivalent sources improves the source reconstruction when using the near field array and, thus improves the far field directivity estimates in the frequency range of interest. The effect of the method is mostly visible when using a small number of sources as the errors decrease significantly, especially at lower frequencies.

The error curve corresponding to the l_1 regularised source distribution over the frequency range of interest is, as expected, located between the one associated with the uniform distribution and the l_1 regularised one for all the various numbers of equivalent sources. The frequencies, where the orange and green curves coincide, are the ones at which the final l_1 regularised source distribution coincides with the ones associated with these single frequencies, while the frequency bands, where there is a deviation between the two curves, are the ones at which the optimum single frequency distribution does not coincide with the one chosen over the whole frequency range, but instead there is another one that can deliver a lower error.

4. Conclusions

In this paper, an application of the inverse method to the indoor synthesis of tyre pass-by noise contribution is studied. The tyre noise contribution is approximated by a 2D-tyre model, which does not take into account the acoustic sources but can be a very good approximation to the vibration of a real car tyre, especially at lower frequencies. The tyre model is then embedded into a model of the acoustic radiation where the far field pressure directivity is synthesised by using a polar array close to the tyre and then compared to the one radiated directly in the far field linear array. Within this method, the equivalent source positions on the tyre circumference are predefined. In the last section, an additional l1-norm regularisation term is used in the inverse method, which optimises the positioning of the equivalent sources by choosing from a number of candidate sources on the tyre circumference. The final optimised far field pressure directivities are compared to the direct and the near-field synthesised ones and it is shown that very small synthesis errors can be achieved in the frequency range of interest with careful selection of the regularisation parameter.

5. Acknowledgements

The authors gratefully acknowledge the European Commission for its support of the Marie Sklodowska Curie program through the ETN PBNv2 project (GA 721615).

REFERENCES

1 International Organization for Standardization, ISO 362-3:2016: Measurement of noise emitted by accelerating road vehicles -- Engineering method -- Part 1: M and N categories, pp. 51.

2 Schuhmacher A., Shirahashi Y., Hirayama M. and Ryu Y., Indoor pass-by noise contribution analysis using source path contribution concept, *Proceedings of the 2012 International Conference on Modal Analysis Noise and Vibration Engineering*, Leuven, Belgium, pp. 3697-3709, (2012).

3 Bianciardi F., Janssens K., Choukri M. and Van Der Auweraer H., Indoor pass-by noise engineering: a motorbike application case, *Proceedings of Inter-Noise 2014*, Melbourne, Australia (2014).

4 Kim U., Maunder M., Grant P. and Mawdsley D., Developing a Car to Meet New Pass-By Noise Requirements using Simulation and Testing, SAE Technical Paper 2015-01-2319, (2015).

5 Chu Z., Wang H., Chen C. and Yan, R. Kang H., Source Path Contribution Analysis for Vehicle Indoor Pass-By Noise, SAE Technical Paper 2017-01-2247, (2017).

6 Janssens K., Aarnoutse P., Gajdatsy P., Britte L., Deblauwe F. and Van der Auwerauer H., Time-Domain Source Contribution Analysis Method for In-Room Pass-by Noise, SAE Technical Paper 2011-01-1609, (2011).

7 Rustighi E. and Elliott S.J., Stochastic road excitation and control feasibility in a 2D linear tyre model, *Journal of Sound and Vibration*, **300** (3-5), 490-501, (2007).

8 Papaioannou A., Elliott S.J. and Cheer J., L_1 regularisation in the inverse method for the synthesis of tyre pass-by noise, *Inter-Noise 2019*, Madrid, Spain, (2019)

9 Huang S. and Soedel W., Effects of coriolis acceleration on the free and forced in-plane vibrations of rotating rings on elastic foundation, *Journal of Sound and Vibration* **115** (2), 253–274, (1987).

10 Holland K.R. and Nelson P.A., The application of inverse methods to spatially-distributed acoustic sources, *Journal of Sound and Vibration* **332**, 5727-5747, (2013).

11 Nelson P.A. and Yoon S.H., Estimation of acoustic source strength by inverse methods: Part 1, conditioning of the inverse problem, *Journal of Sound and Vibration* **233** (4), 643-668, (2000).

12 Hald J., Fast wideband acoustical holography, *Journal of the Acoustical Society of America*, **139** (4), 1508-1057, (2016)

13 Van den Berg E. and Friedlander M.P., SPGL1: A solver for large-scale sparse reconstruction, http://www.cs.ubc.ca/labs/scl/spgl1